



# Measuring Respiration in Isolated Murine Brain Mitochondria: Implications for Mechanistic Stroke Studies

Jared A. Sperling<sup>1</sup> · Siva S. V. P. Sakamuri<sup>1</sup> · Aaron L. Albuck<sup>1,3</sup> · Venkata N. Sure<sup>1</sup> · Wesley R. Evans<sup>1,3</sup> · Nicholas R. Peterson<sup>1</sup> · Ibolya Rutkai<sup>1,3</sup> · Ricardo Mostany<sup>1,3</sup> · Ryoussuke Satou<sup>2</sup> · Prasad V. G. Katakam<sup>1,3</sup> 

Received: 19 April 2019 / Accepted: 29 May 2019 / Published online: 6 June 2019  
© Springer Science+Business Media, LLC, part of Springer Nature 2019

## Abstract

Measuring mitochondrial respiration in brain tissue is very critical in understanding the physiology and pathology of the central nervous system. Particularly, measurement of respiration in isolated mitochondria provides the advantage over the whole cells or tissues as the changes in respiratory function are intrinsic to mitochondrial structures rather than the cellular signaling that regulates mitochondria. Moreover, a high-throughput technique for measuring mitochondrial respiration minimizes the experimental time and the sample-to-sample variation. Here, we provide a detailed protocol for measuring respiration in isolated brain non-synaptosomal mitochondria using Agilent Seahorse XFe24 Analyzer. We optimized the protocol for the amount of mitochondria and concentrations of ADP, oligomycin, and trifluoromethoxy carbonylcyanide phenylhydrazone (FCCP) for measuring respiratory parameters for complex I-mediated respiration. In addition, we measured complex II-mediated respiratory parameters. We observed that 10 µg of mitochondrial protein per well, ADP concentrations ranging between 2.5 and 10 mmol/L along with 5 µmol/L of oligomycin, and 5 µmol/L of FCCP are ideal for measuring the complex I-mediated respiration in isolated mouse brain mitochondria. Furthermore, we determined that 2.5 µg of mitochondrial protein per well is ideal for measuring complex II-mediated respiration. Notably, we provide a discussion of logical analysis of data and how the assay could be utilized to design mechanistic studies for experimental stroke. In conclusion, we provide detailed experimental design for measurement of various respiratory parameters in isolated brain mitochondria utilizing a novel high-throughput technique along with interpretation and analysis of data.

**Keywords** Mitochondrial respiration · Non-synaptosomal mitochondria · Isolated mitochondria · Oxygen consumption rate

## Introduction

The brain consumes 20% of the whole-body energy although it weighs 2% of the body weight indicating the high dependence of neurons on energy (Attwell and Laughlin 2001). Mitochondria generate the majority of ATP required for neurons through oxidative phosphorylation that couples transfer

of electrons from NADH and FADH<sub>2</sub> through the electron transport chain (ETC) to the phosphorylation of ADP to ATP (Golpich et al. 2017). Mitochondrial respiratory dysfunction significantly affects neuronal function and contributes to the pathology of neurological diseases (Golpich et al. 2017). Mutations on either mitochondrial or nuclear DNA leading to deficits in mitochondrial respiratory function have been reported in various neurological diseases including cerebral ataxia and epilepsy (Wang et al. 2019).

Mitochondrial dysfunction is reported to contribute to age-related cognitive impairments and neurodegenerative diseases like Alzheimer's, Parkinson's, amyotrophic lateral sclerosis, and Huntington's diseases (Wang et al. 2019). Thus, evaluating mitochondrial respiratory parameters is a useful method for the study of pathological states and the screening of potential therapeutic agents for neurological disorders. Measuring mitochondrial respiration in intact and permeabilized cells or isolated mitochondria each have

✉ Prasad V. G. Katakam  
pkatakam@tulane.edu

<sup>1</sup> Department of Pharmacology, Tulane University School of Medicine, 1430 Tulane Avenue, New Orleans, LA 70112, USA

<sup>2</sup> Department of Physiology, Tulane University School of Medicine, 1430 Tulane Avenue, New Orleans, LA 70112, USA

<sup>3</sup> Tulane Brain Institute, Tulane University, 200 Flower Hall, New Orleans, LA 70118, USA

merits and drawbacks. Whole cell studies are useful in determining the cellular mechanisms regulating mitochondrial respiration. On the other hand, respiratory measurements in permeabilized cells and isolated mitochondria help to determine intrinsic mitochondrial defects. However, respiratory changes in permeabilized cells could be due to changes in either quality or volume/number of the mitochondria. In contrast, measuring respiration in isolated mitochondria by manipulating various substrates helps in detailed functional characterization of mitochondria that is independent of changes in mitochondrial dynamics.

Compared to the classical electrode-based methods, using high-throughput techniques for assessing mitochondrial respiration in multiple samples within a short time is highly advantageous. Here, we report a protocol to measure respiration in isolated non-synaptosomal mitochondria from mouse brain using Agilent Seahorse XFe24 analyzer. The technique simultaneously measures oxygen consumption rate (OCR) in 20 samples using a fluorometrical method. This high-throughput respirometry technique is widely used in neurons (Agostini et al. 2016). Recent studies have adopted this method to measure mitochondrial respiration from brain sections, hippocampal slices, and permeabilized neurons (Fried et al. 2014; Clerc and Polster 2012; Schuh et al. 2011). Very few studies reported this technique for studying isolated mitochondria from the brain (Long et al. 2015; Sauerbeck et al. 2011; Tyrrell et al. 2017; Andersen et al. 2019; Cebak et al. 2017). Although these methodologies are available for isolated mitochondria from tissues like skeletal muscle and heart, since mitochondria from various tissues differ in their respiratory metabolism, it is ideal to optimize the conditions for each tissue (Boutagy et al. 2015; Sakamuri et al. 2018). However, a detailed protocol/methodology for measuring respiration in isolated brain mitochondria using Agilent Seahorse XFe24 Analyzer is long overdue.

Here, we report a comprehensive protocol for measuring respiratory measurements like state II, III, IIIu, and IVo using complex I (pyruvate/malate) and complex II (succinate/rotenone) substrates in isolated and density-gradient purified non-synaptosomal mitochondria from mouse brain. Basal or state II respiration is the OCR after the addition of substrates without any stimulators or inhibitors of respiration and provides information about the substrate metabolism and respiratory chain activity under the physiological conditions. State III respiration is the maximal OCR observed after the addition of saturating amounts of ADP in the presence of the substrates. State III respiration is influenced by the adenine nucleotide metabolism, substrate utilization, and ETC activity including the oxidative phosphorylation (OXPHOS) (Brand and Nicholls 2011). State IV respiration is the OCR observed after the inhibition of ATP synthase by oligomycin, and represents the proton leak from the inner mitochondrial membrane (Brand and Nicholls 2011).

State IIIu (state III uncoupled) respiration is the maximal OCR observed after the uncoupling of ETC from OXPHOS using uncoupler molecules like trifluoromethoxy carbonylcyanide phenylhydrazone (FCCP). State IIIu respiration is influenced by substrate metabolism and the efficiency of the ETC. Details of potential impairments of substrate metabolism, efficiency of ETC, and mitochondrial ETC activity may be found in reviews in the literature (Nicholls 2001, 2002, 2004, 2005; Nicholls and Budd 1998; Nicholls et al. 1999). We have tested various parameters like the quantity of mitochondria, ADP, oligomycin, and FCCP concentrations to standardize the optimal conditions which have not been reported previously.

## Experimental Design

### Materials

#### 1. Isolation Medium (IM), pH 7.4

Sucrose (225 mmol/L, S3-500, Fisher Scientific, Pennsylvania, USA)

Mannitol (70 mmol/L, M4125, Sigma-Aldrich, Missouri, USA)

HEPES (5 mmol/L, BP310-500, Fisher Scientific, Pennsylvania, USA)

EGTA (1 mmol/L, E-4378, Sigma-Aldrich, Missouri, USA)

Fatty Acid-Free Bovine Serum Albumin, Fraction V (BSA) (0.5%, A7030, Sigma-Aldrich, Missouri, USA)

#### 2. Mitochondrial Assay Buffer (MAS), pH 7.4

Sucrose (225 mmol/L)

Mannitol (70 mmol/L)

HEPES (2 mmol/L,)

EGTA (1 mmol/L)

Magnesium Chloride (5 mmol/L, M9272, Sigma-Aldrich, Missouri, USA)

Potassium Dihydrogen Phosphate (10 mmol/L, P5655, Sigma-Aldrich, Missouri, USA)

Fatty Acid-Free Bovine Serum Albumin (0.2%)

#### 3. Sodium Pyruvate (10 mmol/L, P2256, Sigma-Aldrich, Missouri, USA)

#### 4. *D*-Malic Acid (2 mmol/L, 46940-U, Sigma-Aldrich, Missouri, USA)

#### 5. Percoll Solution, pH 7.4

Percoll (17-0891-01, GE Healthcare, Illinois, USA)  
 Sucrose (225 mmol/L)  
 Mannitol (70 mmol/L)  
 HEPES (5 mmol/L)  
 EGTA (1 mmol/L)

## 6. Mito Stress Test Chemicals

Adenosine 5'-diphosphate sodium salt (A2754, Sigma-Aldrich, Missouri, USA)  
 Oligomycin (495455 – 10 mg, EMD Millipore, Darmstadt, Germany)  
 FCCP (15218, Cayman Chemicals, Michigan, USA)  
 Antimycin A (A8674, Sigma-Aldrich, Missouri, USA)  
 Rotenone (R8875, Sigma-Aldrich, Missouri, USA)

## Procedure

### Animals

Two-month-old C57BL/6 J male mice (Stock No: 000664,  $n = 12$ ) were acquired from Jackson Laboratory (Bar Harbor, Maine). Animals were housed in the vivarium of the Department of Comparative Medicine at Tulane University access to food and water ad libitum. Animal procedures and protocols were approved by the Institutional Animal Care and Use Committee of Tulane University and performed in accordance with the ARRIVE guidelines.

### Mitochondria Isolation

The non-synaptosomal mitochondria from mouse brain were isolated using the method previously reported by us (Busija et al. 2005). Mice were anesthetized with isoflurane (VETOne, Boise, Idaho). The absence of toe pinch reflex was used to check consciousness before euthanized through decapitation. Brain was collected after opening the skull with an incision through the midline. Mouse brain was placed in 10 mL of isolation medium (IM) on ice (in 60 mm petri dish) and the cerebellum and brain stem were removed. It is noted that fresh IM (pH 7.4) was prepared every week and stored at 4 °C. Two cerebral hemispheres were transferred to a separate petri dish with fresh IM and were cut into smaller pieces using fine scissors. Brain tissue in the IM was transferred to a glass rod homogenizer (15 mL tissue grinder, cat# 357544, Wheaton, USA) and the tissue was homogenized by 8–10 gentle strokes with a pestle. Later, the homogenate was transferred to a 50 mL centrifuge tube. We cautiously made sure that negative pressure was not created during the homogenization. The homogenate was centrifuged at 1300×g for 3 min at 4 °C (Eppendorf,

Hamburg, Germany). The supernatant was transferred to a new separate centrifuge tube, and the pellet was resuspended in 5 mL IM. Resuspended pellet was centrifuged again at 1300×g for 3 min, and the supernatant was transferred to the new centrifuge tube. The two supernatants were pooled and centrifuged at 21,000×g for 10 min at 4 °C (DuPont Instruments, Delaware, USA). It is noted that fresh 100% Percoll (pH 7.4) was prepared every week and stored at 4 °C. During this spin, Percoll solutions of 40%, 24%, and 15% were prepared using 100% Percoll solution and IM. 3.5 mL of 24% Percoll was added to a new centrifuge tube. Beneath the 24% Percoll at the bottom of the centrifuge tube, 4.5 mL of 40% Percoll was added slowly. A visible interface was noticed to be present between the two gradients layered in the tube. The supernatant was removed from the centrifuged homogenate. Subsequently, the pellet was dissolved in 3.5 mL of 15% Percoll solution and was slowly layered on top of the Percoll gradient prepared as described above. The mitochondrial pellets were gently resuspended at all the steps using appropriate tips that were cut at the end (to decrease the pressures during mixing). To resuspend the pellet, 10–20 gentle pipetting was applied. The sample was centrifuged at 30,000×g for 8 min at 4 °C. A layer of non-synaptosomal mitochondria was observed between the 40% and 24% Percoll gradient layers. The mitochondrial layer was collected by a 5 mL BD syringe and spinal needle (catalogue# 405182) and was transferred to a new centrifuge tube and 5 mL of IM was added. Notably, the mitochondrial layer was collected gently with wide gauge spinal needle to prevent mechanical damage to mitochondria. The solution was centrifuged at 16,000×g for 10 min at 4 °C. The pellet generated from this spin was found to be loose in consistency. We used 5 mL, 1 mL, and 200 µL pipettes to remove the supernatant as much as possible. Later, 0.5 mL of BSA solution was added (10 mg/mL in IM) to the pellet and the centrifuge tube was gently tapped to resuspend the mitochondrial pellet in the BSA solution. Next, 4.5 mL of IM was added to the mitochondrial suspension and was mixed by gently pipetting. The mitochondrial suspension was centrifuged at 7000×g for 10 min at 4 °C. Later, the supernatant was discarded, and the mitochondrial pellet was resuspended in 100–200 µL of IM based on the pellet size. The mitochondrial suspension was kept on ice until the mito stress test assay was ready. Importantly, isolation of mitochondria took 2.5–3 h. For optimal results, the isolated mitochondria were used for analysis within 3–4 h after the isolation. The protein concentration in the sample was measured using appropriate protein assay kits. It is noted that the sample was diluted 10–20 times for the measurements with similarly diluted IM as the blank.

## Mito Stress Test Assay

**XF Calibration Plate and Cartridge Preparation** XF calibration plate was prepared the day before the assay. 1 mL of XF calibration buffer was added to the XF sensor cartridge and incubated overnight at 37 °C in the non-CO<sub>2</sub> incubator. On the day of the assay, required amount of the MAS was prepared either with pyruvate (10 mmol/L) and malate (2 mmol/L), for complex I assay, or succinate (10 mmol/L) and rotenone (2 μmol/L) for complex II assay, using 2X MAS, ultrapure water, and respective stock solutions. The pH was adjusted to 7.4. Notably, 2X MAS (pH 7.4) was prepared and store at 4 °C for up to a month. Stocks of sodium pyruvate (10 mmol/L), succinate (10 mmol/L), and malate (2 mmol/L) were prepared in MAS and the pH was adjusted to 7.4. Later, aliquots of stocks were stored at –20 °C. MAS with appropriate substrates (complex I or II) was used to prepare the ADP stock solution (50 mmol/L) and the pH was adjusted to 7.4 using 1 N KOH. ADP stocks were stored at 4 °C and used within a week. MAS with complex I or complex II substrates was used to dilute the stock solutions of mito stress compounds, including oligomycin (50 μmol/L) and FCCP (50 μmol/L). Antimycin A and rotenone mix (100 μmol/L and 20 μmol/L) were prepared for complex I assays or just antimycin A (100 μmol/L) for complex II assays. It is noted that 10 mmol/L stock solutions of oligomycin, FCCP, antimycin, and rotenone were prepared in 95% ethyl alcohol. Aliquots were prepared and stored at –20 °C. Calibrated cartridge was loaded with the ADP and mito stress compounds. Port A: ADP (22 μL); Port B: Oligomycin (24 μL); Port C: FCCP (26 μL); Port D: Antimycin A and rotenone (28 μL) (for complex I assays & just antimycin A (28 μL) for complex II assays). The final concentration of drugs to which mitochondria were to be exposed diluted ten times than the second stock solutions: ADP (5 mmol/L), oligomycin (5 μmol/L), FCCP (5 μmol/L), and antimycin (10 μmol/L) and rotenone (2 μmol/L). The protocol design for the Seahorse analyzer used in the study is shown in Table 1. The cartridge was placed (after taking out the pink plate) in the analyzer and was calibrated (calibration took 20–30 min).

**Mitochondrial Loading to the Cell Culture Plate** Mitochondria were diluted to the desired final concentration (0.2 μg/μL) using MAS with complex I or complex II substrates. 50 μL of MAS was loaded in the wells A1, C3, B4, and D6, as blanks. 50 μL of the mitochondrial dilution was loaded into the remaining wells (10 μg protein per well). Cell culture microplate was centrifuged at 2000×g for 20 min at 4 °C. After the centrifugation, 150 μL of MAS was added along the walls to all the wells slowly and the mitochondria were incubated in a non-CO<sub>2</sub> incubator for 10 min. Once the calibration was completed, calibration plate was exchanged

**Table 1** Seahorse assay protocol

Command	Time	Compound
Equilibration	12 min	
Mix	1 min	
Wait	3 min	
Measure	3 min	
Mix	1 min	
Wait	3 min	
Measure	3 min	
Inject Port A		ADP <sup>a</sup>
Mix	1 min	
Measure	6 min	
Inject Port B		Oligomycin
Mix	1 min	
Measure	3 min	
Inject Port C		FCCP
Mix	1 min	
Measure	3 min	
Inject Port D		Antimycin A + Rotenone
Mix	1 min	
Measure	6 min	

<sup>a</sup>Measurement time can be decreased to 3 min if using low concentrations of the ADP

with the cell culture microplate containing the mitochondria and the assay was run with the predesigned protocol. Notably, mitochondrial solution was mixed gently before loading the wells in the cell culture plate to achieve homogenous distribution of mitochondria across the wells.

**Data Analysis** To view the results of the assay, “Overview” mode with “standard error of the mean” (Wave 2.3.0) was selected. Blank well that shows higher OCR value affecting the values of the test samples was deselected. The data were exported into an excel file and arrangement of the OCR data of the various measurements were produced (basal 1, basal 2, ADP, oligomycin, FCCP, antimycin A/rotenone) in a new sheet as per the various treatments or the groups. The average of all basal OCR values was taken for the control group and this value was used to normalize all the OCR values of the plate (i.e., relative OCR data). This method was used for processing the data from all the plates in the experiment. The average of all the technical replicates was taken for all the relative OCR data for each plate. The average of “basal 1” and “basal 2” readings was taken as basal OCR or state II respiration. Values of ADP, oligomycin, and FCCP were taken as state III, state IV<sub>o</sub>, and state III<sub>u</sub> respiration, respectively. The respiratory control ratios (RCR) were calculated from point-to-point graphs. The ratio of highest reading after the ADP

addition (state III) and lowest point after the oligomycin addition (state IV<sub>o</sub>) was designated as RCR value. Five technical replicates for each treatment or group, and data from 6 to 10 mice per group provided the power to detect significant differences between groups, if they exist.

## Results

### Protein Concentration

Basal, or state II, state III, state IV<sub>o</sub>, state III<sub>u</sub>, and non-ETC-associated mitochondrial OCRs were increased in a dose-dependent manner with the mitochondrial protein concentration and maximal OCRs were observed with 10  $\mu\text{g}$  of protein per well (Figs. 1, 2). It is expected that the presence of more mitochondria increases the OCR due to increased substrate utilization.

### ADP Concentration

Addition of ADP increased the mitochondrial respiration (state III) linearly and saturated at specific ADP concentration. We observed similar state III respiration at the three different ADP concentrations (2.5 mmol/L, 5.0 mmol/L, and 10.0 mmol/L) tested, indicating that the concentrations we used were well above the optimal ADP required to elicit the maximal respiration (Fig. 3).

### Oligomycin Concentration

We observed similar state IV<sub>o</sub> respiration with 1 and 2.5  $\mu\text{mol/L}$  concentrations ( $464.8 \pm 36.7$  and  $475.9 \pm 62.2$  pmol of  $\text{O}_2/\text{min}$ , respectively), and it is further decreased with 5 and 10  $\mu\text{mol/L}$  ( $212.5 \pm 26.5$  and  $168.6 \pm 22.9$  pmol of  $\text{O}_2/\text{min}$ , respectively, Fig. 4).

### FCCP Concentration

We observed gradual increase in state III<sub>u</sub> respiration with FCCP concentration and we observed maximal OCR at 5  $\mu\text{mol/L}$  concentration (Fig. 5). Interestingly, we observed a decrease in state III<sub>u</sub> at 10  $\mu\text{mol/L}$  FCCP, which is expected as irrecoverable decrease in membrane potential leads to significant decrease in respiration (Fig. 5).

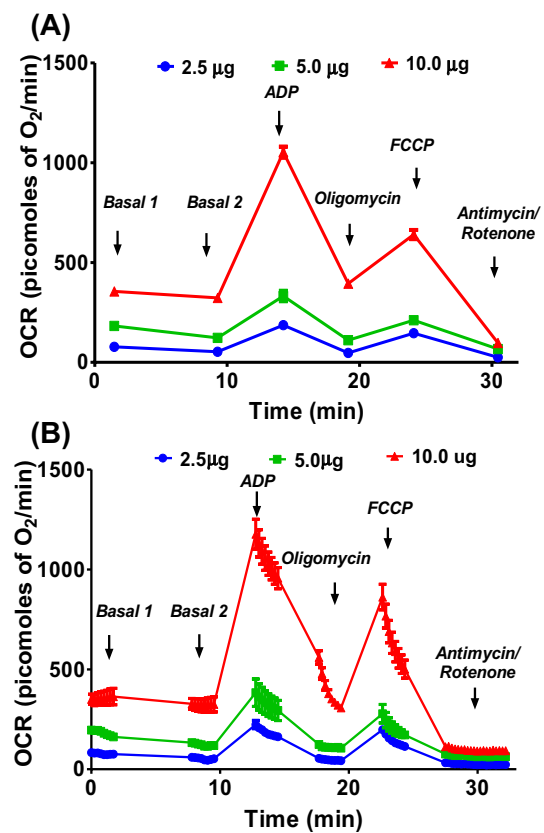


**Fig. 1** Optimizing protein concentration for complex I respiratory measurements in isolated mouse brain non-synaptosomal mitochondria using Seahorse XFe24 Analyzer. Isolated mouse (C57BL/6 J) non-synaptosomal mitochondria at various concentrations (2.5, 5, and 10  $\mu\text{g}$  protein/well) were treated with ADP (5 mmol/L), oligomycin (5  $\mu\text{mol/L}$ ), FCCP (5  $\mu\text{mol/L}$ ), and antimycin (10  $\mu\text{mol/L}$ )/rotenone (2  $\mu\text{mol/L}$ ) combination in the presence of complex 1 substrates (pyruvate, 10 mmol/L and malate, 2 mmol/L) and oxygen consumption rate (OCR) was measured. **a** Representative plot of mid-point OCR data. **b** Representative plot of point-to-point OCR. Data expressed as mean  $\pm$  SEM ( $n = 5$  wells/group)

### Complex II-Driven Respiration

Like complex I-driven respiration, complex II-driven OCRs were increased in a dose-dependent manner with the protein concentration (Figs. 6, 7). Based on the data, 2.5  $\mu\text{g}$  of mitochondrial protein was optimal for complex II-driven respiratory measurements, as higher doses appeared to greatly increase state IV<sub>o</sub> respiration while state III respiration increased to as much as 1500 pmol of  $\text{O}_2/\text{min}$  (Figs. 6, 7).

### RCR Measurements

RCR was calculated from the point-to-point data by taking the ratio between the highest OCR point after ADP injection

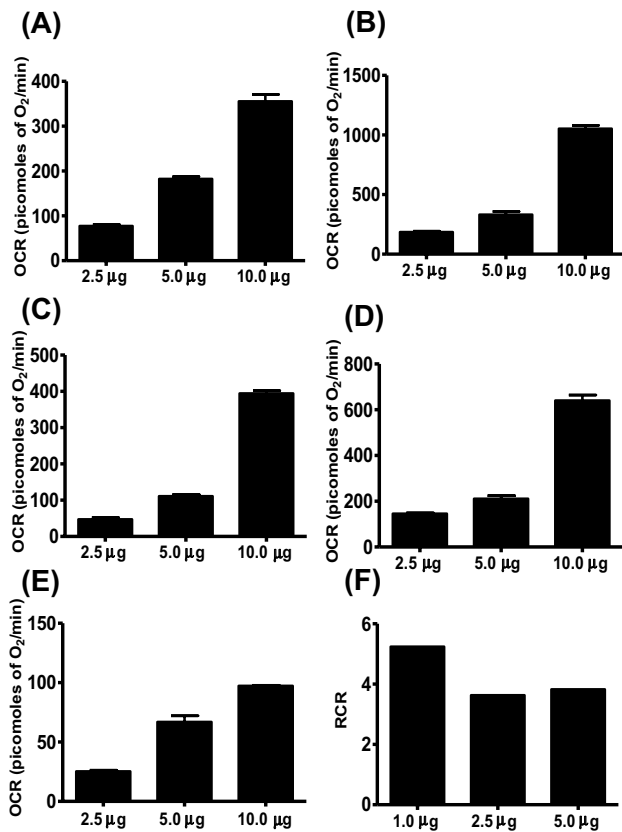


**Fig. 2** Optimizing protein concentration for complex I respiratory measurements in isolated mouse brain non-synaptosomal mitochondria using Seahorse XFe24 Analyzer. Isolated mouse (C57BL/6 J) non-synaptosomal mitochondria at various concentrations (1, 2.5, 5, and 10 µg protein/well) were treated with ADP (5 mmol/L), oligomycin (5 µmol/L), FCCP (5 µmol/L), and antimycin (10 µmol/L)/rotenone (2 µmol/L) combination in the presence of complex I substrates (pyruvate, 10 mmol/L and malate, 2 mmol/L) and oxygen consumption rate (OCR) was measured. **a** State II or basal respiration. **b** State III respiration. **c** State IV<sub>o</sub> respiration. **d** State III<sub>u</sub> respiration. **e** Antimycin/rotenone. **f** Respiratory control ratio (state III/IV<sub>o</sub>). Data expressed as mean ± SEM ( $n = 5$  wells/group)

and the lowest point after the oligomycin injection (state III/IV<sub>o</sub>). RCR values were between 3.5 and 5 for both the complex assays (Fig. 2, 7).

## Discussion

In the present study, we optimized the conditions for measuring respiration in isolated mitochondria from mouse brain using Seahorse XFe24 analyzer (Fig. 8). We observed OCR at basal state (state II), followed by an increase in OCR with ADP addition (state III). At later steps, we noticed a decrease in OCR with oligomycin (state IV<sub>o</sub>) followed by an increase with FCCP addition (state III<sub>u</sub>). Finally, OCR was abolished to the minimum with the addition of antimycin

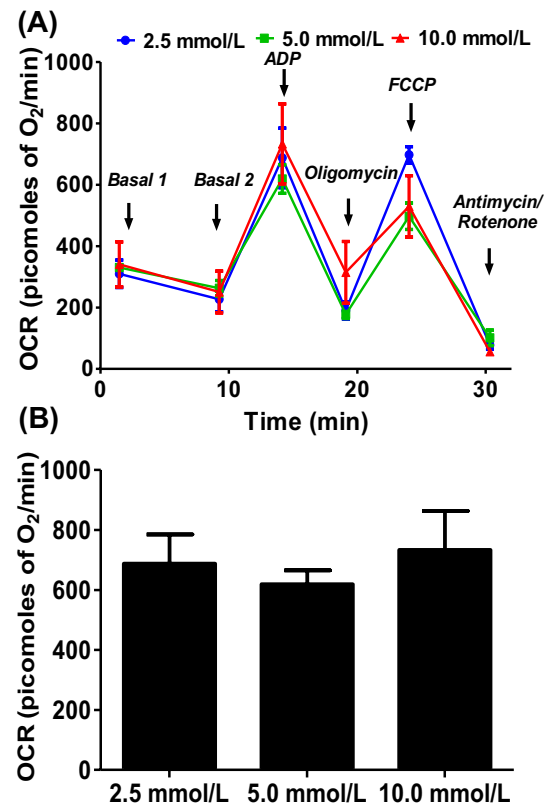


**Fig. 3** Optimizing ADP concentration for measuring state III respiration in isolated mouse brain non-synaptosomal mitochondria using Seahorse XFe24 Analyzer. Isolated mouse (C57BL/6 J) non-synaptosomal mitochondria (10 µg protein/well) were treated with various concentrations of ADP (2.5, 5, and 10 mmol/L), oligomycin (5 µmol/L), FCCP (5 µmol/L), and antimycin (10 µmol/L)/rotenone (2 µmol/L) combination in the presence of complex I substrates (pyruvate, 10 mmol/L and malate, 2 mmol/L), and oxygen consumption rate (OCR) was measured. **a** Representative plot of mid-point OCR data. **b** State III respiration. Data expressed as mean ± SEM ( $n = 5$  wells/group)

A/rotenone. We observed a similar trend in all the experiments suggesting uniformly intact mitochondria preparations, adequate substrate, and inhibitor concentrations as well as other critical experimental conditions. Furthermore, respiratory control ratio (RCR) value, which is a marker of mitochondrial quality, was found to be between 3.5 and 5 indicating that mitochondrial preparations are functionally intact and efficient in coupling oxidation to generation of ATP by phosphorylation.

Optimal mitochondrial concentration is an important determinant of the measurement of OCR as too little amount of mitochondria may not consume enough oxygen to be detected reliably while too many mitochondria may run out of substrates and ADP for oxidative phosphorylation. We consider 10 µg is the optimal protein concentration to measure respiration in isolated murine non-synaptosomal mitochondria using Seahorse XFe24 analyzer due to the higher

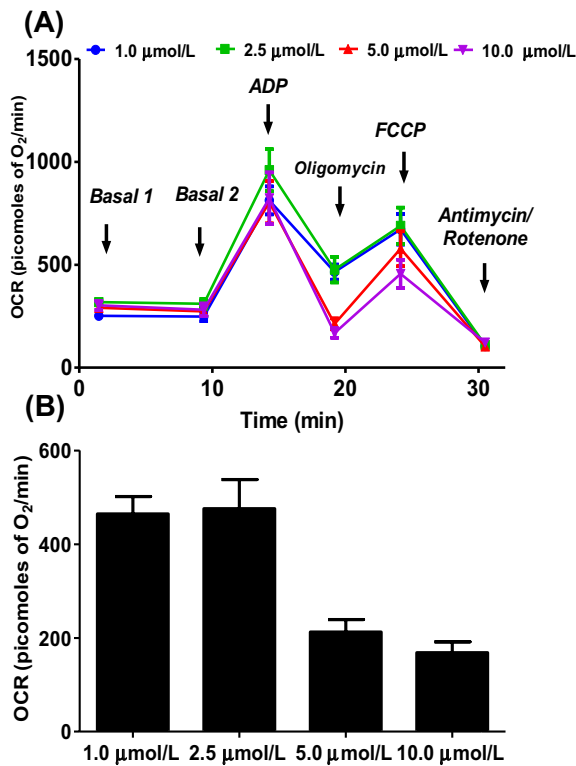


**Fig. 4** Optimizing oligomycin concentration for measuring state IVo respiration in isolated mouse brain non-synaptosomal mitochondria using Seahorse XFe24 Analyzer. Isolated mouse (C57BL/6 J) non-synaptosomal mitochondria (10 μg protein/well) were treated with ADP (10 mmol/L), various doses of oligomycin (1, 2.5, 5, and 10 μmol/L), FCCP (5 μmol/L), and antimycin (10 μmol/L)/rotenone (2 μmol/L) combination in the presence of complex 1 substrates (pyruvate, 10 mmol/L and malate, 2 mmol/L), and oxygen consumption rate (OCR) was measured. **a** Representative plot of mid-point OCR data. **b** State IVo respiration. Data expressed as mean ± SEM ( $n=5$  wells/group)

state III and state IIIu respiration values obtained. Another important determinant of optimization is the ADP concentration, we suggest using ADP concentrations between 2.5 and 10 mmol/L for the assays of mitochondrial respiration. Notably, ADP concentration should always be considered together with mitochondrial protein concentration.

Oligomycin decreases the OCR (state IVo) by inhibiting ATP synthase in inner mitochondrial membrane, thus decreasing the flow of protons into the mitochondrial matrix. Though we observed approximately similar state IVo respiration with 5 and 10 μmol/L oligomycin, we prefer to use 5 μmol/L as we observed better FCCP-induced respiration with this dose compared to the 10 μmol/L concentration. We speculate that a complete blockade of ATP synthase may promote a robust FCCP-induced enhancement of OCR. Thus, attention should be paid to the FCCP-induced respiration for each concentration of oligomycin tested during optimization of mitochondrial respiration.

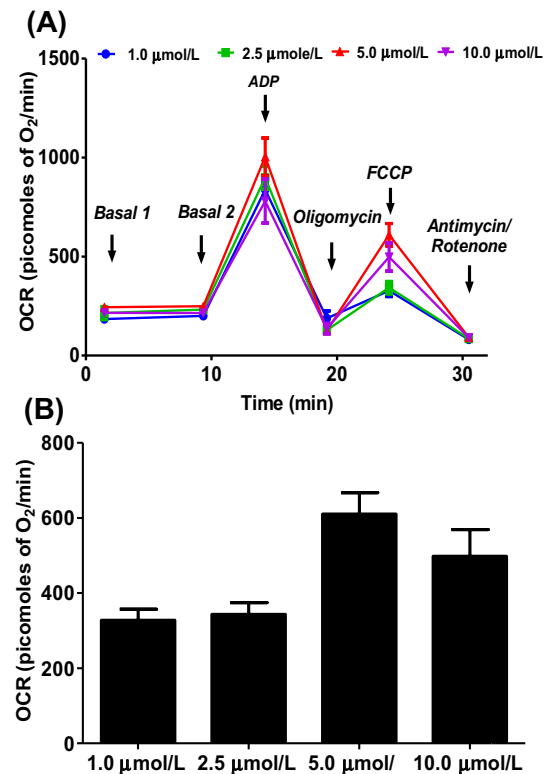


**Fig. 5** Optimizing FCCP (trifluoromethoxy carbonylcyanide phenylhydrazine) concentration for measuring state IIIu (state III uncoupled) respiration in isolated mouse brain non-synaptosomal mitochondria using Seahorse XFe24 Analyzer. Isolated mouse (C57BL/6 J) non-synaptosomal mitochondria (10 μg protein/well) were treated with ADP (10 mmol/L), oligomycin (10 μmol/L), various doses of FCCP (1, 2.5, 5, and 10 μmol/L), and antimycin (10 μmol/L)/rotenone (2 μmol/L) combination in the presence of complex 1 substrates (pyruvate, 10 mmol/L and malate, 2 mmol/L), and oxygen consumption rate (OCR) was measured. **a** Representative plot of mid-point OCR data. **b** State IIIu respiration. Data expressed as mean ± SEM ( $n=5$  wells/group)

FCCP is an ionophore that depolarizes the inner mitochondrial membrane resulting in stimulation of electron transport through mitochondrial electron transport chain thereby OCR to the maximal extent in order to maintain the proton gradient across the inner mitochondrial membrane. As explained above, OCR responses to FCCP treatment have to be considered together with protein and oligomycin concentrations for the purpose of optimization of mitochondrial respiration assays.

Compared to OCRs with complex I substrate-driven respiration, OCR following respiration driven by complex II substrates will be higher at any given concentration. Hence, we utilized fewer mitochondria when respiration was measured in the presence of complex II substrates compared to that of the complex I substrates. It is likely that higher OCRs could deplete oxygen levels in the wells leading to erroneous measurements of respiratory parameters as shown

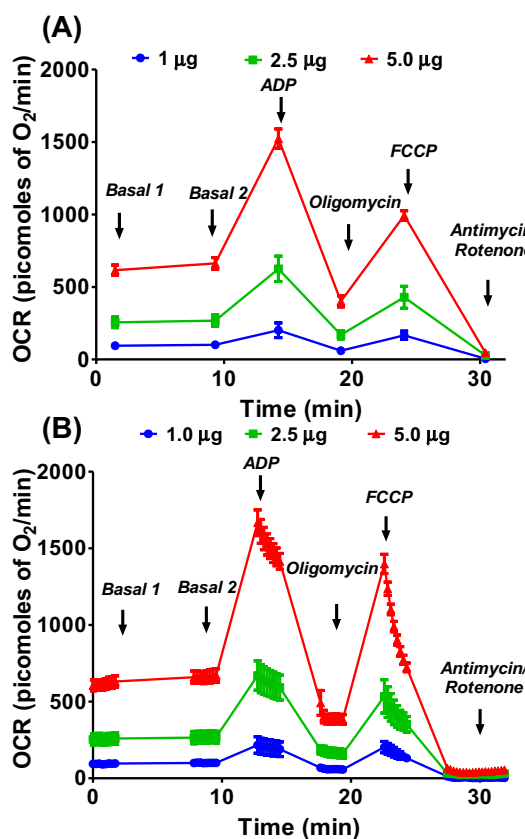


**Fig. 6** Optimizing protein concentration for Complex II respiratory measurements in isolated mouse brain non-synaptosomal mitochondria using Seahorse XFe24 Analyzer. Isolated mouse (C57BL/6 J) non-synaptosomal mitochondria at various concentrations (1, 2.5, and 5 µg protein/well) were treated with ADP (5 mmol/L), oligomycin (5 µmol/L), FCCP (5 µmol/L), and antimycin (10 µmol/L) combination in the presence of complex 2 substrate succinate (10 mmol/L) and rotenone (2 µmol/L). Oxygen consumption rates (OCR) were measured. **a** Representative plot of mid-point OCR data. **b** Representative plot of point-to-point OCR. Data expressed as mean  $\pm$  SEM ( $n=5$  wells/group)

previously (Rogers et al. 2011). Furthermore, using 5 µg of mitochondrial protein per well for complex II-based respiration assays may not be suitable in case the compound being tested increases state III or state IIIu respiration, as it will completely deplete the oxygen in the wells leading to erroneous results.

RCR values are often used as indicator of the quality of mitochondria as increased OCR leading to increased generation of ATP from ADP reflects the ability of mitochondria to efficiently use the substrates and carry out the function of meeting the energy demands of the cell. Typically, RCR values between 3.5 and 5 are consistent with the values reported in the literature and indicate functionally intact mitochondrial preparations with efficiently coupled oxidative phosphorylation (Rogers et al. 2011).

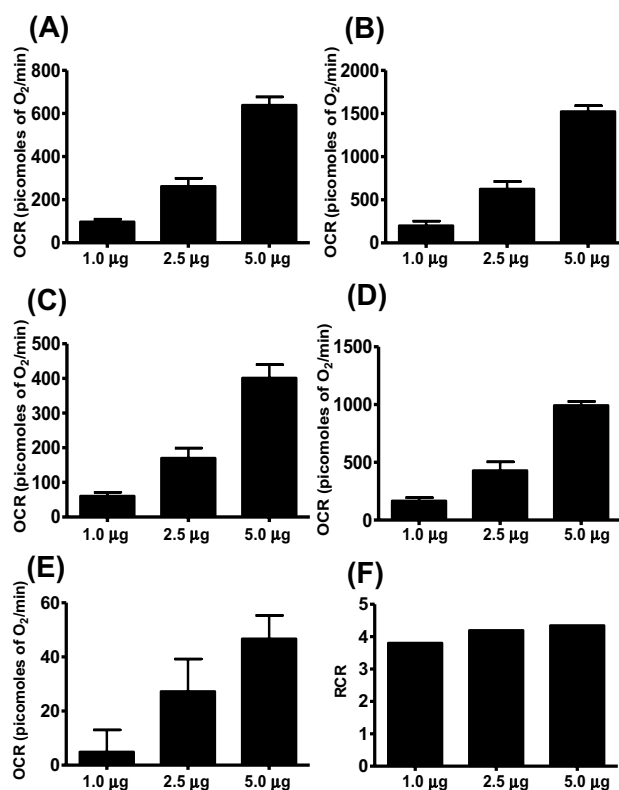
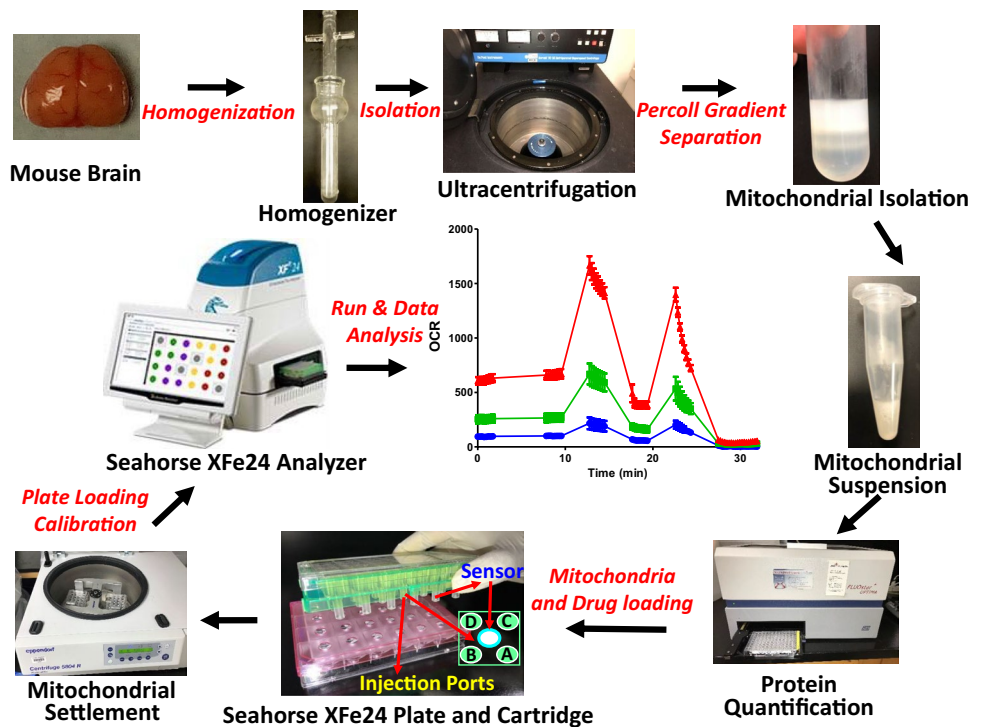


**Fig. 7** Optimizing protein concentration for Complex II respiratory measurements in isolated mouse brain non-synaptosomal mitochondria using Seahorse XFe24 Analyzer. Isolated mouse (C57BL/6 J) non-synaptosomal mitochondria at various concentrations (1, 2.5, and 5 µg protein/well) were treated with ADP (5 mmol/L), oligomycin (5 µmol/L), FCCP (5 µmol/L), and antimycin (10 µmol/L) combination in the presence of complex 2 substrate succinate (10 mmol/L) and rotenone (2 µmol/L). Oxygen consumption rates (OCRs) were measured. **a** State II or basal respiration. **b** State III respiration. **c** State IVO respiration. **d** State IIIu respiration. **e** Antimycin/rotenone. **f** Respiratory control ratio (state III/IVo). Data expressed as mean  $\pm$  SEM ( $n=5$  wells/group)

Though we provided the protocol for measuring respiratory parameters related to complex I and complex II, researchers can measure the similar parameters for complex III and IV using selective substrates. Glycerol-3-phosphate (20 mM) or duroquinol (0.6 mM) can be used to measure complex III activities, whereas tetramethyl-p-phenylenediamine (TMPD, 0.2 mmol/L) can be used for complex IV activities in the presence of ascorbic acid (10 mM) that is required to keep TMPD in the reduced state (Barrientos et al. 2009).

Thus, we optimized the mitochondrial content, ADP concentration, and other mito stress test pharmacological agents to measure the respiration in isolated mouse brain non-synaptosomal mitochondria using Seahorse XFe24 analyzer, as described in the present detailed protocol for the assay. In addition to the complex I-mediated respiration, we

**Fig. 8** A flow diagram of the method is provided for the benefit of easy understanding of the protocol



optimized the amount of mitochondria needed to measure the complex II-mediated respiration.

### Implications for Stroke Research

Occlusion of major cerebral artery induces complex cellular changes. Fall of blood flow in the core or focal tissue following arterial occlusion results in disruption of glucose and oxygen delivery leading to greatly diminished ATP generation (Back et al. 2004; Belayev et al. 1997; Memezawa et al. 1992; Zhao et al. 1997). Contributions to perfusion from the adjacent artery tissues surrounding ischemic core result in less ischemic ‘penumbral’ or perifocal’ regions comprised of electrically silent hyperpolarized neurons (Back et al. 2004; Hossmann 1994; Memezawa et al. 1992). The differences in the severity of ischemia in the core and penumbra induce diverse mechanisms of cellular injury and cell death. As oxidative phosphorylation is the major source of ATP production (92%) in neurons, mitochondria are the critical players in tissue injury and death during a stroke (Russo et al. 2018), when ATP production is reduced due to the forced switch to anaerobic metabolism. Mitochondrial dysfunction mediates stroke-induced neuronal injury and death, and recent studies have reported the possible therapeutic potential of healthy mitochondria to minimize stroke injury (Russo et al. 2018). The majority of studies have proposed the role of mitochondrial dynamics, ROS production, apoptosis, and mitophagy in cerebral ischemia-associated neuronal death, but very few studies addressed the respiratory

defects at the mitochondrial level (Yang et al. 2018; Nakai et al. 1997; Kuroda et al. 1996; Pandya et al. 2011). Nakai et al. have reported secondary mitochondrial dysfunction in the focal region after ischemia–reperfusion as evidenced by decreased ADP and uncoupler-induced mitochondrial respiration (Nakai et al. 1997). Similar changes have also been reported in the penumbra region (Kuroda et al. 1996). These studies were performed in rats using crude tissue homogenates and purified mitochondria. Very recent studies reported similar results in mice, and they compared the mitochondrial respiratory between contralateral and ischemic cerebral hemispheres, but not between the focal and penumbra regions (Novgorodov et al. 2016; Berressem et al. 2016; Schwarzkopf et al. 2013).

Requirement of higher amounts of isolated mitochondria (in milligrams) by traditional methods might be one of the reasons for using the rat model of the stroke instead of mice for respiratory measurements. Though some studies were conducted in mice, whole cerebral hemispheres were used for mitochondrial preparation instead of brain regions vulnerable to ischemia and the penumbra that is jeopardized by ischemia and yet salvageable (Schwarzkopf et al. 2013; Berressem et al. 2016; Novgorodov et al. 2016). Using high-throughput techniques like Seahorse XFe24, mitochondrial respiration can be studied simultaneously in multiple samples using micrograms of mitochondria. This translates into characterizing purified mitochondria from various regions of the mouse brain or comparing mitochondria from various transgenic animals. Notably, comparison of mitochondrial

**Table 2** Comparison between the various protocols using isolated mitochondria applying different instruments

Parameters	Classical clarke oxygen electrode (Moreira et al. 2003)	High-resolution respirometer (Oroboros O2 k) (Takahashi et al. 2018)	Seahorse XFe24 analyzer (current protocol)
Oxygen detection	Polarography based	Polarography based	Fluorescence based
Mitochondrial quantity used for the assay (measured as protein)	800 µg	100–300 µg	1–10 µg
Mitochondrial respiration medium volume	1 mL	2 mL	200 µL
Number of samples measured	One	Two	Twenty
Replicates	One after the other	Duplicates at a time	Multiple replicates may be used ( $n = 2–20$ ) based on the experimental design
Drug injections	Manual	Manual	Automatic
Number of injections	Multiple	Multiple	Maximum of four
Number of drugs	Multiple	Multiple	Multiple
Time between the isolation and the assay across the samples	Laborious to maintain the constant time	Laborious to maintain the constant time	Constant time can be maintained easily
Additional parameters other than OCR	No	pH, hydrogen peroxide, membrane potential, ATP, calcium ions, and various molecules measured when coupled with fluorimeter	Extracellular acidification rate (ECAR)

We compared the published protocols in terms of quantity of the mitochondria used. The present protocol requires significantly lower quantity of mitochondria for OCR measurements compared to the protocols using Clarke oxygen electrode and high-resolution respirometer

respiration in regions of the brain with varying susceptibility to ischemic injury could yield mechanistic data helpful for identifying therapeutic targets for stroke. Reduced ATP generation following ischemic-injury results in dissipation of ionic gradients across the plasma membrane leading to dramatic loss of intracellular potassium and influx of calcium into cells (Doyle et al. 2008; Gido et al. 1997; Kristian et al. 1998; Sims and Muyderman 2010). Several therapeutic agents have been proposed to be neuroprotective by activating mitochondrial ion channels (Busija et al. 2005; Domoki et al. 2004; Gaspar et al. 2009, 2008; Mayanagi et al. 2007; Piwonska et al. 2016; Shimizu et al. 2002) and studies in isolated mitochondria are helpful in high-throughput screening of potential therapeutic agents against stroke. Furthermore, as previous methods could simultaneously measure mitochondrial respiration in limited number of samples, it is laborious to isolate multiple fresh mitochondrial preparations for the individual measurements requiring multiple mice, introducing higher technical variations into data acquisition. For better understanding of advantages and the disadvantages, we compared between the protocols that measured respiration in isolated brain mitochondria using various methods including classical Clark oxygen electrode, high-resolution respirometer, and Seahorse XFe24 analyzer (Table 2).

Thus, Seahorse XFe24 technology allows mitochondrial functional studies from small quantity of mitochondria, sampling of many regions of brain, and yet requiring

limited number of animals. In summary, we described a novel high-throughput assay to measure respiration in the isolated brain mitochondria that has the ability to provide mitochondria-based mechanistic data to study potential therapies for stroke.

**Acknowledgements** We thank Ms. Sufen Zheng for her technical help for the studies.

**Funding** This research project was supported by the National Institutes of Health: National Institute of Neurological Disorders and Stroke and National Institute of General Medical Sciences (NS094834—P.V. Katakam), National Institute on Aging (R01AG047296—R. Mostany), and National Institute of Diabetes and Digestive and Kidney Diseases (DK107694—R. Satou). In addition, the study was supported by American Heart Association (National Center Scientist Development Grant, 14SDG20490359—P.V. Katakam; Greatersoutheast Affiliate Predoctoral Fellowship Grant, 16PRE27790122—V.N. Sure; and Scientist Development Grant, 17SDG33410366—I. Rutkai), Louisiana Clinical and Translational Science Center (supported in part by U54 GM104940 from the National Institute of General Medical Sciences of the National Institutes of Health, which funds the LACaTS to I. Rutkai), and Louisiana Board of Regents grants (RCS, LEQSF(2016-19)-RD-A-24—R. Mostany). This work was supported in part by [U54 GM104940] from the National Institute of General Medical Sciences of the National Institutes of Health, which funds the Louisiana Clinical and Translational Science Center (to I. Rutkai). The content is solely the responsibility of the authors and does not necessarily represent the official views of the National Institutes of Health.

## Compliance with Ethical Standards

**Conflict of interest** The authors declare that they have no conflict of interest.

**Ethical Approval** Animal procedures and protocols were approved by the Institutional Animal Care and Use Committee of Tulane University and performed in accordance with the ARRIVE guidelines. Furthermore, the manuscript is in compliance with the ethical standards and the policies of the journal.

## References

- Agostini, M., Romeo, F., Inoue, S., Niklison-Chirou, M. V., Elia, A. J., Dinsdale, D., et al. (2016). Metabolic reprogramming during neuronal differentiation. *Cell Death and Differentiation*, 23(9), 1502–1514. <https://doi.org/10.1038/cdd.2016.36>.
- Andersen, J. V., Jakobsen, E., Waagepetersen, H. S., & Aldana, B. I. (2019). Distinct differences in rates of oxygen consumption and ATP synthesis of regionally isolated non-synaptic mouse brain mitochondria. *Journal of Neuroscience Research*. <https://doi.org/10.1002/jnr.24371>.
- Attwell, D., & Laughlin, S. B. (2001). An energy budget for signaling in the grey matter of the brain. *Journal of Cerebral Blood Flow and Metabolism*, 21(10), 1133–1145. <https://doi.org/10.1097/00004647-200110000-00001>.
- Back, T., Hemmen, T., & Schuler, O. G. (2004). Lesion evolution in cerebral ischemia. *Journal of Neurology*, 251(4), 388–397. <https://doi.org/10.1007/s00415-004-0399-y>.
- Barrientos, A., Fontanesi, F., & Diaz, F. (2009). Evaluation of the mitochondrial respiratory chain and oxidative phosphorylation system using polarography and spectrophotometric enzyme assays. *Current Protocols in Human Genetics, Chapter, 19*(Unit19), 13. <https://doi.org/10.1002/0471142905.hg1903s63>.
- Belayev, L., Zhao, W., Busto, R., & Ginsberg, M. D. (1997). Transient middle cerebral artery occlusion by intraluminal suture: I. Three-dimensional autoradiographic image-analysis of local cerebral glucose metabolism-blood flow interrelationships during ischemia and early recirculation. *Journal of Cerebral Blood Flow and Metabolism*, 17(12), 1266–1280. <https://doi.org/10.1097/00004647-199712000-00002>.
- Berressem, D., Koch, K., Franke, N., Klein, J., & Eckert, G. P. (2016). Intravenous treatment with a long-chain omega-3 lipid emulsion provides neuroprotection in a murine model of ischemic stroke—A pilot study. *PLoS ONE*, 11(11), e0167329. <https://doi.org/10.1371/journal.pone.0167329>.
- Boutagy, N. E., Rogers, G. W., Pyne, E. S., Ali, M. M., Hulver, M. W., & Frisard, M. I. (2015). Using isolated mitochondria from minimal quantities of mouse skeletal muscle for high throughput microplate respiratory measurements. *Journal of Visualized Experiments*. <https://doi.org/10.3791/53216>.
- Brand, M. D., & Nicholls, D. G. (2011). Assessing mitochondrial dysfunction in cells. *Biochemical Journal*, 435(2), 297–312. <https://doi.org/10.1042/BJ20110162>.
- Busija, D. W., Katakam, P., Rajapakse, N. C., Kis, B., Grover, G., Domoki, F., et al. (2005). Effects of ATP-sensitive potassium channel activators diazoxide and BMS-191095 on membrane potential and reactive oxygen species production in isolated piglet mitochondria. *Brain Research Bulletin*, 66(2), 85–90. <https://doi.org/10.1016/j.brainresbull.2005.03.022>.
- Cebak, J. E., Singh, I. N., Hill, R. L., Wang, J. A., & Hall, E. D. (2017). Phenelzine protects brain mitochondrial function in vitro and in vivo following traumatic brain injury by scavenging the reactive carbonyls 4-hydroxynonenal and acrolein leading to cortical histological neuroprotection. *Journal of Neurotrauma*, 34(7), 1302–1317. <https://doi.org/10.1089/neu.2016.4624>.
- Clerc, P., & Polster, B. M. (2012). Investigation of mitochondrial dysfunction by sequential microplate-based respiration measurements from intact and permeabilized neurons. *PLoS ONE*, 7(4), e34465. <https://doi.org/10.1371/journal.pone.0034465>.
- Domoki, F., Bari, F., Nagy, K., Busija, D. W., & Siklos, L. (2004). Diazoxide prevents mitochondrial swelling and Ca<sup>2+</sup> accumulation in CA1 pyramidal cells after cerebral ischemia in newborn pigs. *Brain Research*, 1019(1–2), 97–104. <https://doi.org/10.1016/j.brainres.2004.05.088>.
- Doyle, K. P., Simon, R. P., & Stenzel-Poore, M. P. (2008). Mechanisms of ischemic brain damage. *Neuropharmacology*, 55(3), 310–318. <https://doi.org/10.1016/j.neuropharm.2008.01.005>.
- Fried, N. T., Moffat, C., Seifert, E. L., & Oshinsky, M. L. (2014). Functional mitochondrial analysis in acute brain sections from adult rats reveals mitochondrial dysfunction in a rat model of migraine. *The American Journal of Physiology-Cell Physiology*, 307(11), C1017–C1030. <https://doi.org/10.1152/ajpcell.00332.2013>.
- Gaspar, T., Domoki, F., Lenti, L., Katakam, P. V., Snipes, J. A., Bari, F., et al. (2009). Immediate neuronal preconditioning by NS1619. *Brain Research*, 1285, 196–207. <https://doi.org/10.1016/j.brainres.2009.06.008>.
- Gaspar, T., Katakam, P., Snipes, J. A., Kis, B., Domoki, F., Bari, F., et al. (2008). Delayed neuronal preconditioning by NS1619 is independent of calcium activated potassium channels. *Journal of Neurochemistry*, 105(4), 1115–1128. <https://doi.org/10.1111/j.1471-4159.2007.05210.x>.
- Gido, G., Kristian, T., & Siesjo, B. K. (1997). Extracellular potassium in a neocortical core area after transient focal ischemia. *Stroke*, 28(1), 206–210.
- Golpich, M., Amini, E., Mohamed, Z., Azman Ali, R., Mohamed Ibrahim, N., & Ahmadiani, A. (2017). Mitochondrial dysfunction and biogenesis in neurodegenerative diseases: Pathogenesis and treatment. *CNS Neuroscience & Therapeutics*, 23(1), 5–22. <https://doi.org/10.1111/cns.12655>.
- Hossmann, K. A. (1994). Viability thresholds and the penumbra of focal ischemia. *Annals of Neurology*, 36(4), 557–565. <https://doi.org/10.1002/ana.410360404>.
- Kristian, T., Gido, G., Kuroda, S., Schutz, A., & Siesjo, B. K. (1998). Calcium metabolism of focal and penumbral tissues in rats subjected to transient middle cerebral artery occlusion. *Experimental Brain Research*, 120(4), 503–509.
- Kuroda, S., Katsura, K., Hillered, L., Bates, T. E., & Siesjo, B. K. (1996). Delayed treatment with alpha-phenyl-N-tert-butyl nitron (PBN) attenuates secondary mitochondrial dysfunction after transient focal cerebral ischemia in the rat. *Neurobiology of Disease*, 3(2), 149–157.
- Long, A. N., Owens, K., Schlappal, A. E., Kristian, T., Fishman, P. S., & Schuh, R. A. (2015). Effect of nicotinamide mononucleotide on brain mitochondrial respiratory deficits in an Alzheimer's disease-relevant murine model. *BMC Neurology*, 15, 19. <https://doi.org/10.1186/s12883-015-0272-x>.
- Mayanagi, K., Gaspar, T., Katakam, P. V., Kis, B., & Busija, D. W. (2007). The mitochondrial K(ATP) channel opener BMS-191095 reduces neuronal damage after transient focal cerebral ischemia in rats. *Journal of Cerebral Blood Flow and Metabolism*, 27(2), 348–355. <https://doi.org/10.1038/sj.jcbfm.9600345>.
- Memezawa, H., Minamisawa, H., Smith, M. L., & Siesjo, B. K. (1992). Ischemic penumbra in a model of reversible middle cerebral artery occlusion in the rat. *Experimental Brain Research*, 89(1), 67–78.
- Moreira, P. I., Santos, M. S., Moreno, A. M., Seica, R., & Oliveira, C. R. (2003). Increased vulnerability of brain mitochondria in diabetic (Goto-Kakizaki) rats with aging and amyloid-beta exposure. *Diabetes*, 52(6), 1449–1456.

- Nakai, A., Kuroda, S., Kristián, T., & Siesjö, B. K. (1997). The immunosuppressant drug FK506 ameliorates secondary mitochondrial dysfunction following transient focal cerebral ischemia in the rat. *Neurobiology of Disease*, 4(3), 288–300. <https://doi.org/10.1006/nbdi.1997.0146>.
- Nicholls, D. (2002). Mitochondrial bioenergetics, aging, and aging-related disease. *Science of Aging Knowledge Environment*, 2002(31), pe12. <https://doi.org/10.1126/sageke.2002.31.pe12>.
- Nicholls, D. G. (2001). A history of UCP1. *Biochemical Society Transactions*, 29(Pt 6), 751–755.
- Nicholls, D. G. (2004). Mitochondrial membrane potential and aging. *Aging Cell*, 3(1), 35–40. <https://doi.org/10.1111/j.1474-9728.2003.00079.x>.
- Nicholls, D. G. (2005). Mitochondria and calcium signaling. *Cell Calcium*, 38(3–4), 311–317. <https://doi.org/10.1016/j.ceca.2005.06.011>.
- Nicholls, D. G., & Budd, S. L. (1998). Mitochondria and neuronal glutamate excitotoxicity. *Biochimica et Biophysica Acta*, 1366(1–2), 97–112.
- Nicholls, D. G., Budd, S. L., Ward, M. W., & Castilho, R. F. (1999). Excitotoxicity and mitochondria. *Biochemical Society Symposium*, 66, 55–67.
- Novgorodov, S. A., Riley, C. L., Keffler, J. A., Yu, J., Kindy, M. S., Macklin, W. B., et al. (2016). SIRT3 deacetylates ceramide synthases: Implications for mitochondrial dysfunction and brain injury. *Journal of Biological Chemistry*, 291(4), 1957–1973. <https://doi.org/10.1074/jbc.M115.668228>.
- Pandya, J. D., Sullivan, P. G., & Pettigrew, L. C. (2011). Focal cerebral ischemia and mitochondrial dysfunction in the TNF $\alpha$ -transgenic rat. *Brain Research*, 1384, 151–160. <https://doi.org/10.1016/j.brainres.2011.01.102>.
- Piwonska, M., Szewczyk, A., Schroder, U. H., Reymann, K. G., & Bednarczyk, I. (2016). Effectors of large-conductance calcium-activated potassium channel modulate glutamate excitotoxicity in organotypic hippocampal slice cultures. *Acta Neurobiologiae Experimentalis (Wars)*, 76(1), 20–31.
- Rogers, G. W., Brand, M. D., Petrosyan, S., Ashok, D., Elorza, A. A., Ferrick, D. A., et al. (2011). High throughput microplate respiratory measurements using minimal quantities of isolated mitochondria. *PLoS ONE*, 6(7), e21746. <https://doi.org/10.1371/journal.pone.0021746>.
- Russo, E., Napoli, E., & Borlongan, C. V. (2018). Healthy mitochondria for stroke cells. *Brain Circulation*, 4(3), 95–98. [https://doi.org/10.4103/bc.bc\\_20\\_18](https://doi.org/10.4103/bc.bc_20_18).
- Sakamuri, S., Sperling, J. A., Sure, V. N., Dholakia, M. H., Peterson, N. R., Rutkai, I., et al. (2018). Measurement of respiratory function in isolated cardiac mitochondria using Seahorse XFe24 Analyzer: Applications for aging research. *Geroscience*, 40(3), 347–356. <https://doi.org/10.1007/s11357-018-0021-3>.
- Sauerbeck, A., Pandya, J., Singh, I., Bittman, K., Readnower, R., Bing, G., et al. (2011). Analysis of regional brain mitochondrial bioenergetics and susceptibility to mitochondrial inhibition utilizing a microplate based system. *Journal of Neuroscience Methods*, 198(1), 36–43. <https://doi.org/10.1016/j.jneumeth.2011.03.007>.
- Schuh, R. A., Clerc, P., Hwang, H., Mehrabian, Z., Bittman, K., Chen, H., et al. (2011). Adaptation of microplate-based respirometry for hippocampal slices and analysis of respiratory capacity. *Journal of Neuroscience Research*, 89(12), 1979–1988. <https://doi.org/10.1002/jnr.22650>.
- Schwarzkopf, T. M., Hagl, S., Eckert, G. P., & Klein, J. (2013). Neuroprotection by bilobalide in ischemia: Improvement of mitochondrial function. *Pharmazie*, 68(7), 584–589.
- Shimizu, K., Lacza, Z., Rajapakse, N., Horiguchi, T., Snipes, J., & Busija, D. W. (2002). MitoK(ATP) opener, diazoxide, reduces neuronal damage after middle cerebral artery occlusion in the rat. *American Journal of Physiology-Heart and Circulatory Physiology*, 283(3), H1005–H1011. <https://doi.org/10.1152/ajpheart.00054.2002>.
- Sims, N. R., & Muyderman, H. (2010). Mitochondria, oxidative metabolism and cell death in stroke. *Biochimica et Biophysica Acta*, 1802(1), 80–91. <https://doi.org/10.1016/j.bbadis.2009.09.003>.
- Takahashi, K., Miura, Y., Ohsawa, I., Shirasawa, T., & Takahashi, M. (2018). In vitro rejuvenation of brain mitochondria by the inhibition of actin polymerization. *Scientific Reports*, 8(1), 15585. <https://doi.org/10.1038/s41598-018-34006-5>.
- Tyrrell, D. J., Bharadwaj, M. S., Jorgensen, M. J., Register, T. C., Shively, C., Andrews, R. N., et al. (2017). Blood-based bioenergetic profiling reflects differences in brain bioenergetics and metabolism. *Oxidative Medicine and Cellular Longevity*, 2017, 7317251. <https://doi.org/10.1155/2017/7317251>.
- Wang, Y., Xu, E., Musich, P. R., & Lin, F. (2019). Mitochondrial dysfunction in neurodegenerative diseases and the potential countermeasure. *CNS Neuroscience & Therapeutics*. <https://doi.org/10.1111/cns.13116>.
- Yang, J. L., Mukda, S., & Chen, S. D. (2018). Diverse roles of mitochondria in ischemic stroke. *Redox Biology*, 16, 263–275. <https://doi.org/10.1016/j.redox.2018.03.002>.
- Zhao, W., Belayev, L., & Ginsberg, M. D. (1997). Transient middle cerebral artery occlusion by intraluminal suture: II. Neurological deficits, and pixel-based correlation of histopathology with local blood flow and glucose utilization. *Journal of Cerebral Blood Flow and Metabolism*, 17(12), 1281–1290. <https://doi.org/10.1097/00004647-199712000-00003>.

**Publisher's Note** Springer Nature remains neutral with regard to jurisdictional claims in published maps and institutional affiliations.